EMBO reports

scientific report

The role of trimerization in the osmoregulated betaine transporter BetP

Camilo Perez[1], Kamil Khafizov[2], Lucy R. Forrest[2+], Reinhard Krämer[3] & Christine Ziegler[1++]

[1]Department of Structural Biology, Max-Planck Institute of Biophysics, Frankfurt am Main, [2]Computational Structural Biology Group, Max-Planck Institute of Biophysics, Frankfurt am Main, and [3]Institut of Biochemistry, University of Cologne, Köln, Germany

The osmoregulated betaine transporter BetP is a stable trimer. Structural studies have shown that individual protomers can adopt distinct transport conformations, implying a functional role for the trimeric state in transport, although the role of trimerization in regulation is not yet understood. We designed putative monomeric mutants by molecular-dynamics simulations and *in silico* alanine-scanning mutagenesis. Several mutants including BetP-W101A/T351A were monomeric in detergent as well as in the membrane, as shown by blue native gel electrophoresis, crosslinking and electron microscopy. This monomeric form retains the ability to accumulate betaine, but is no longer regulated by hyperosmotic shock.

Keywords: betaine transport; conformational changes; electron microscopy; oligomerization; osmoregulation

EMBO *reports* (2011) **12**, 804–810. doi:10.1038/embor.2011.102

INTRODUCTION

BetP is an efficiently regulated secondary transporter for betaine that is involved in the hyperosmotic stress response (Farwick *et al*, 1995). BetP performs transport catalysis (betaine uptake) and stress stimulus sensing (perception of stress and intramolecular signal transduction), and adapts the transport activity to the extent of the hyperosmotic stress (Ziegler *et al*, 2010). One osmotic stress stimulus is an increase in cytoplasmic K^+ concentration, which is sensed by the 55-residue-long carboxy-terminal domain of BetP (Peter *et al*, 1998; Schiller *et al*, 2004a; Ott *et al,* 2008), a key component in regulating transport activity. BetP adopts the so-called LeuT-fold (Yamashita *et al*, 2005), which is shared by several other transporter families (Forrest *et al*, 2011). However, BetP contains several additional unique features. On the periplasmic side, the amphipathic helix 7 (h7) connects two structurally related repeats, whereas TM2 encloses the transporter core similarly to a stabilizing belt. In addition, the C-terminal domain forms a long α-helix that extends into the cytoplasm. BetP is a trimer in the membrane of two-dimensional crystals, as well as in solubilized form in detergent micelles and in three-dimensional crystals (Ziegler *et al*, 2004; Ressl *et al*, 2009). Interactions between protomers in the trimer involve the structural elements mentioned above. Structural data obtained from two-dimensional crystals shows that each protomer in the BetP trimer adopts a distinct conformational state (Tsai *et al*, 2011), implying coupling between protomers during the transport cycle. In the X-ray crystal structure, the C-terminal helix interacts through a cluster of positively charged residues with negatively charged residues in the cytoplasmic loops of adjacent protomers (Ressl *et al*, 2009). Thus, the structural data indicate a functional role for the trimeric state in enabling cross-talk between protomers, affecting both catalytic and regulatory cycles.

Here, we report structural and biochemical data that demonstrate a functional role for the BetP trimer in both transport and regulation. To design a monomeric mutant protein, we first identified key interfacial residues by molecular-dynamics simulations and *in silico* alanine-scanning mutagenesis calculations. We show that double and triple mutants of key positions yielded the monomeric form of BetP in detergent solution, in proteoliposomes and in *Escherichia coli* cells. Combined with uptake measurements in proteoliposomes and cells, our data support the crucial role of the trimer during both transport and transport regulation. Thus, BetP requires the trimeric state to properly respond to osmotic stress.

RESULTS

Molecular-dynamics simulations

To investigate the molecular interactions responsible for maintaining the trimeric state of BetP, we carried out 30- to 50-ns-long molecular-dynamics simulations of BetP trimers in a hydrated POPG bilayer (Fig 1A). The trimeric protein is stable in these simulations. Thus, for three repeat simulations with different initial velocities, the average root-mean-square deviation of the

[1]Department of Structural Biology, Max-Planck Institute of Biophysics, Frankfurt am Main 60438,
[2]Computational Structural Biology Group, Max-Planck Institute of Biophysics, Frankfurt am Main 60438,
[3]Institut of Biochemistry, University of Cologne, Zülpicher Strasse 47, Köln 50674, Germany
[+]Corresponding author. Tel: +49 6963031600; Fax: +49 6963031502; E-mail: lucy.forrest@biophys.mpg.de
[++]Corresponding author. Tel: +49 6963033054; Fax: +49 6963032209; E-mail: christine.ziegler@biophys.mpg.de

Received 17 February 2011; revised 4 May 2011; accepted 6 May 2011; published online 17 June 2011

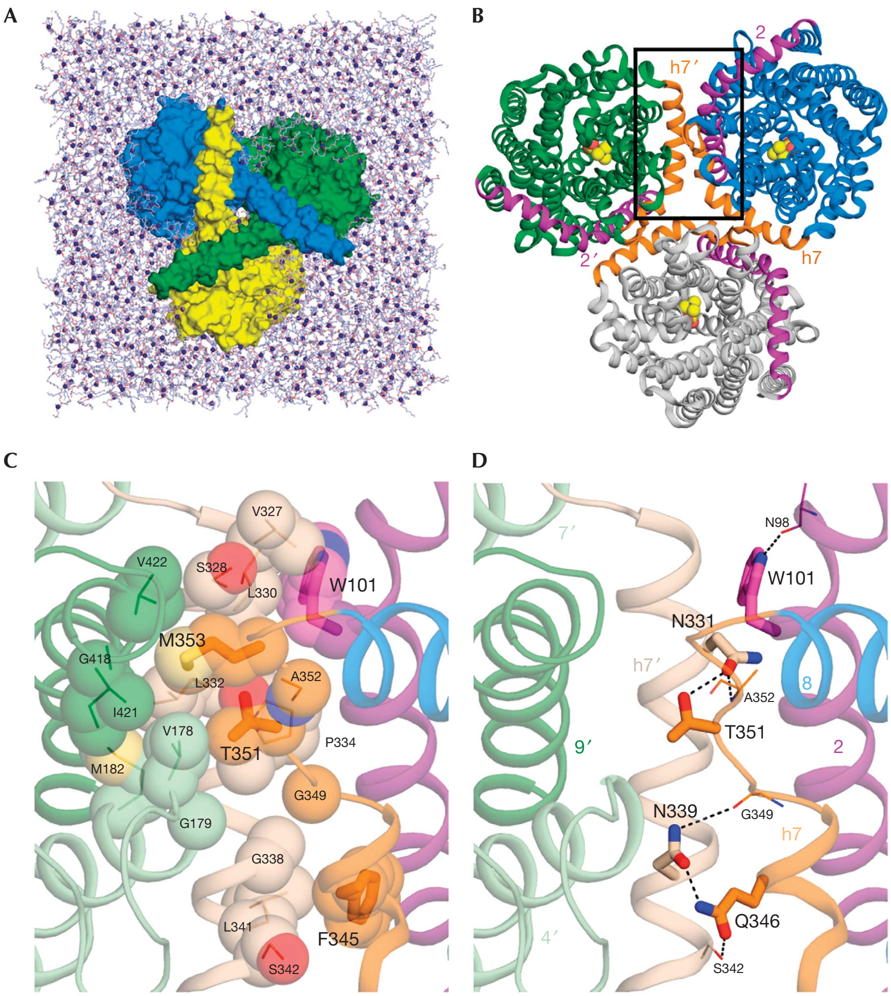

Fig 1 | The structure of BetP and the simulation system. (**A**) The BetP trimer (surface representation) in a POPG lipid bilayer (sticks, with P atoms as spheres), viewed from the cytoplasm, showing the way in which the carboxy-terminal helices crossover to adjacent protomers. Water molecules and ions are omitted for clarity. (**B**) View of the BetP trimer from the periplasm. Helices at the trimer interface are shown in purple (TM2) or orange (h7); those belonging to the upper-left protomer are labelled 2′ and h7′, respectively. Bound betaine molecules are shown (spheres). (**C,D**) Close-up view of the protomer interface in a snapshot of a molecular-dynamics simulation, in the region marked with a box in (**B**), highlighting hydrophobic (**C**) or polar (**D**) interactions. Helices of two adjacent protomers (green and blue in **B**) are shown: h7 (beige), TM9 (dark green), TM4 and TM7 (pale green) from one protomer (labelled h7′, 4′, 7′ and 9′), and h7/L7-8 (orange), TM2 (purple) and TM8 (blue) from the second protomer. Side chains of hot-spot residues identified using *in silico* alanine scanning are shown (thick sticks, large labels), along with their primary interaction partners (thin sticks), and relevant inter-protomer hydrogen bonds are indicated (dashed lines). Residues involved in hydrophobic interactions are shown as spheres (**C**).

Cα atoms in the transmembrane helices from the starting structure are low: 1.6 ± 0.1, 1.7 ± 0.1 and 1.6 ± 0.1 Å. The individual protomers in the trimer are similarly stable, as is the monomeric protein in separate simulations (supplementary Fig S1 online). Furthermore, in the latter simulations, no significant destabilization of the helices at the interfacial region was observed (supplementary Fig S1 online), suggesting that a stable monomeric construct of BetP is possible.

In silico alanine scanning

We then calculated the binding free energy on *in silico* mutation of the interfacial residues to alanine, in the X-ray structure and in several snapshots from the molecular-dynamics trajectories (supplementary Table S1 online). Twenty-three residues were identified as interfacial, nine of which increased the binding free energy ($\Delta\Delta G_{\mathrm{bind}}$) of the protomers by more than 1 kcal/mol on replacement by alanine. Six of these nine residues (bold in supplementary Table S1 online) are located in the horizontal h7 (residues 326–350) or in the loop connecting h7 to TM8 (L7–8; 351–356), indicating that this is the most crucial interfacial region. Indeed, these residues form extensive interactions with adjacent protomers (Fig 1B–D). Between two protomers A and B, e.g. $T351^{A}$ forms hydrogen bonds with $N331^{B}$ or $N339^{B}$ and van der Waals interactions with $V178^{B}$, $G179^{B}$, $M182^{B}$, $L332^{B}$ or $G335^{B}$. Similarly, $F345^{A}$ forms hydrophobic interactions with the side chains of residues $L341^{B}$, $S342^{B}$ or $G338^{B}$.

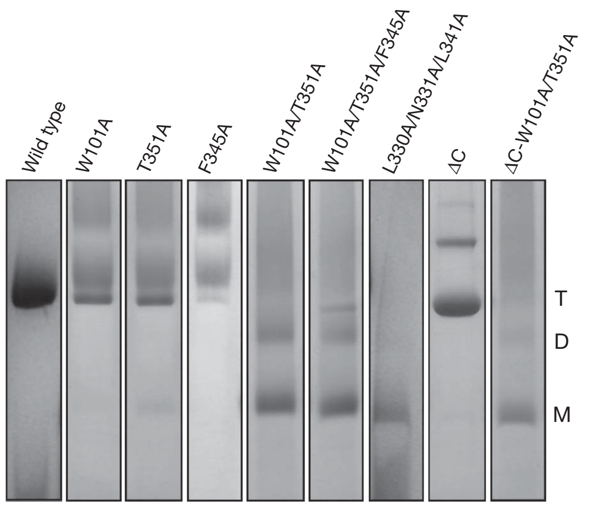

Fig 2 | Mobility of wild-type BetP and mutants in BN–PAGE. Gel lanes are shown separately for viewing purpose; the complete gel and the molecular marker are shown in supplementary Fig S2 online. BN–PAGE, blue native polyacrylamide gel electrophoresis; D, dimer; M, monomer; T, trimer.

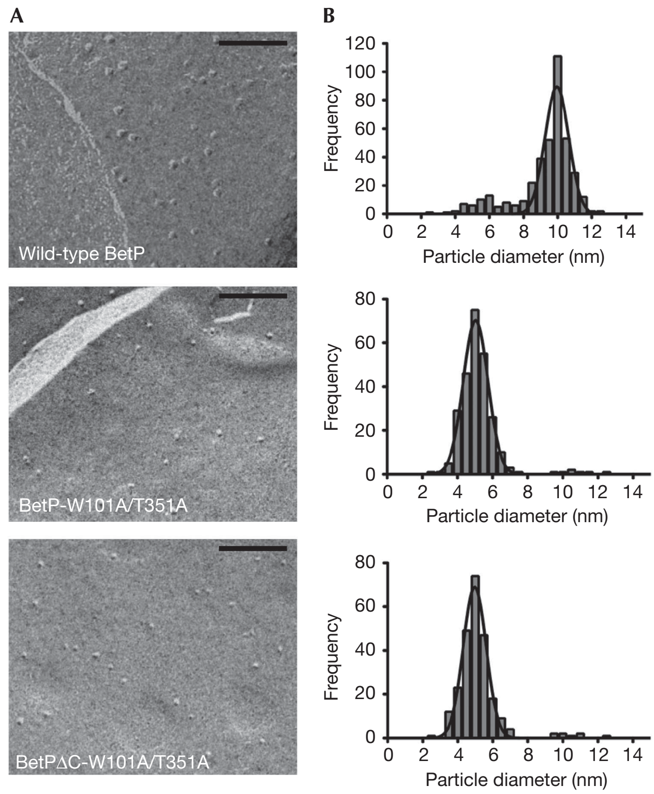

Fig 3 | Results of freeze-fracture electron microscopy. **(A)** Electron micrographs of membrane-reconstituted wild-type BetP and mutants. Scale bar, 100 nm. **(B)** Distribution, that is, number of particles counted as a function of particle size. The line in each plot corresponds to a fit to a Gaussian function.

Several residues from TM2 were also found to be energetically crucial for forming the interface (supplementary Table S1 online). The residue from TM2 most strongly affected by *in silico* mutation was W101, which formed hydrophobic contacts with residues of h7 from another protomer during the simulations (V327, L330 and occasionally L333 and P334; Fig 1C). Finally, two residues of the C-terminal helix, E552 and R568, were significantly affected by *in silico* alanine mutation (supplementary Table S1 online). However, the C-terminally truncated mutant of BetP was found to be trimeric in detergent solution, similarly to the wild-type protein (Tsai *et al*, 2011), indicating that the interactions between the C-terminal helices are not essential for trimer formation.

Disruption of the BetP trimer

On the basis of the *in silico* alanine scanning, several residues were selected for replacement in an attempt to create a monomeric form of BetP. Only residues from h7, L7–8 or TM2 were considered. We first selected W101, for which the effect of *in silico* mutation was the largest (supplementary Table S1 online). We also considered T351 and F345, because $\Delta\Delta G_{\mathrm{bind}}$ was also large for these residues, and because together they are evenly distributed along the length of the interface (Fig 1C,D).

W101, T351 and F345 were replaced by alanine both in the wild type and in a truncated form of BetP that lacks the last 45 residues of its C-terminal domain (BetPΔC). As shown by blue native–polyacrylamide gel electrophoresis (BN-PAGE; Fig 2; supplementary Fig S2 online), although wild-type BetP exclusively forms trimers and dimers of trimers in detergent solution, the mutants BetP-W101A/T351A and BetP-W101A/F345A/T351A predominantly exist as monomers and, to a lesser extent, dimers. The mutant BetP-L330A/N331A/L341A, in which the interaction partners of residues W101, F345 and T351 (Fig 1C,D) have been replaced by alanine, was also mainly monomeric in BN-PAGE (Fig 2). Similarly to wild-type BetP, the truncated protein BetPΔC was found to be trimeric by BN-PAGE, confirming that the C-terminal domain is not crucial for trimer formation (Fig 2). When the same mutations that disrupt the wild-type trimer were introduced into BetPΔC, they again resulted in monomers (Fig 2; supplementary Fig S2 online).

The oligomerization state of wild-type BetP and mutants was further evaluated by size-exclusion chromatography (supplementary Fig S3 online). In the chromatographic profiles, wild-type BetP and the mutant BetP-T351A elute at similar volumes, whereas the mutant BetP-W101A/T351A appears in a 2 ml delayed peak, consistent with the smaller size expected for the monomer.

Wild-type BetP and the mutants BetP-T351A, BetP-W101A/T351A and BetPΔC-W101A/T351A were then reconstituted into *E. coli* polar lipid liposomes, and their oligomeric state in the membrane was analysed by freeze-fracture electron microscopy (Fig 3; supplementary Fig S4 online). The mean particle diameters and areas are shown in Table 1, and their size distribution is shown in Fig 3B and supplementary Fig S4B online. Wild-type BetP and BetP-T351A are mainly trimeric in the membrane of proteoliposomes, whereas the double and triple mutants are mainly monomeric (approximately 95% monomers and approximately 5% a mixture of trimers and dimers).

We tested the effect of the nonspecific crosslinking agent glutaraldehyde on wild-type BetP and on the monomeric mutant BetP-W101A/T351A in detergent solution (Fig 4A). Although the

Table 1 | Freeze-fracture particle analysis of BetP wild-type, BetP-W101A/T351A and BetPΔC-W101A/T351A

	Density (particles/μm²)	Diameter (nm)*	Area (nm²)‡
BetP WT	368.0 ± 15.0	10.0 ± 0.8	78.5 ± 0.5
BetP-W101A/T351A	331.0 ± 19.0	5.1 ± 0.7	20.4 ± 0.4
BetPΔC-W101A/T351A	295.0 ± 12.0	5.0 ± 0.7	19.6 ± 0.4

*Diameters were corrected for the thickness of the platinum–carbon film by subtracting 2.5 ± 0.8 nm from the mean diameters obtained from the frequency histograms; ‡Cross-sectional area was obtained by assuming a circular geometry for the particles. WT, wild type.

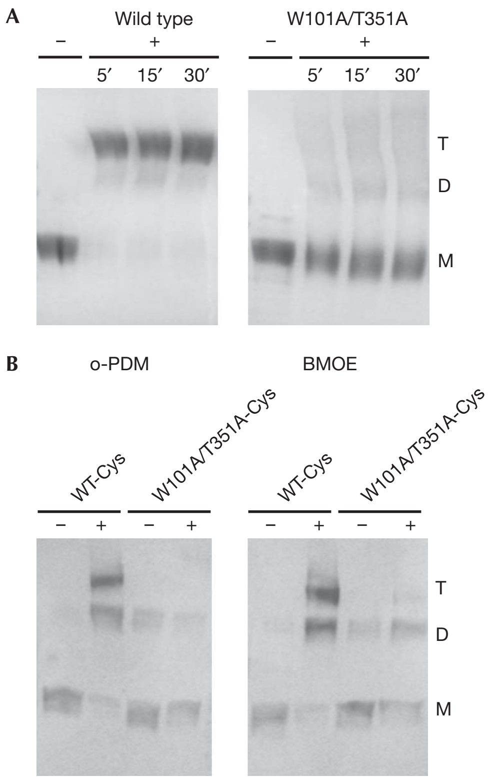

Fig 4 | Crosslinking of BetP. (**A**) Glutaraldehyde crosslinking of detergent solubilized wild-type BetP and BetP-W101A/T351A, shown in a Coomassie-stained 10% SDS–PAGE. Samples were incubated with 0.13% glutaraldehyde (+) for the indicated times, up to 30 min. The control is indicated by –. (**B**) Western blot of BetP-D97C/S328C (WT-Cys) and BetP-D97C/W101A/S328C/T351A (W101A/T351A-Cys) in membrane vesicles of *Escherichia coli* cells. + indicates incubation with 5 mM of o-phenylenedimaleimide (o-PDM) or *bis*-maleimidoethane (BMOE). D, dimer; M, monomer; PAGE, polyacrylamide gel electrophoresis; T, trimer; WT, wild type.

wild-type protein is trimeric in the presence of the crosslinking agent, the BetP-W101A/T351A mutant shows only monomers.

Furthermore, we analysed the oligomeric state of double-cysteine mutants in the membrane of *E. coli* cells by site-directed intermolecular crosslinking (Fig 4B). Two cysteine residues (D97C and S328C, supplementary Fig S5 online) were introduced into the

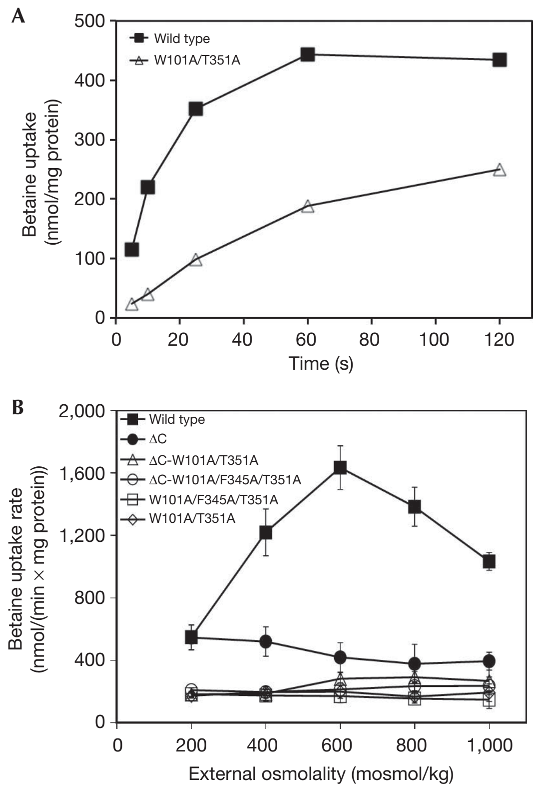

Fig 5 | Measurement of [^{14}C]-betaine uptake rates in proteoliposomes. (**A**) Representative uptake of [^{14}C]-betaine in proteoliposomes with wild-type BetP or the mutant BetP-W101A/T351A at 400 mosml/kg. (**B**) The wild-type BetP activation profile is compared with those of BetPΔC, BetP-W101A/T351A, BetP-W101A/F345A/T351A, BetPΔC-W101A/T351A and BetPΔC-W101A/F345A/T351A. Each value represents the average of three independent measurements. Error bars indicate the standard deviation.

monomeric BetP-W101A/T351A mutant (BetP W101A/T351A-Cys) and into wild-type BetP (BetP WT-Cys). *E. coli* membrane vesicles containing either of the double-cysteine mutants were incubated in the presence of the homo-bifunctional crosslinkers o-phenylenedimaleimide and *bis*-maleimidoethane, which form rigid spacers of approximately 6 and approximately 8 Å, respectively. BetP WT-Cys in the presence of crosslinking agents resulted in a trimeric product, whereas almost no crosslinking could be observed for the monomeric BetP W101A/T351A-Cys (Fig 4B), indicating that in the native *E. coli* membranes the monomers are too far apart to crosslink.

Betaine transport by monomeric BetP mutants

We assayed sodium-driven transport of [^{14}C]-betaine by the monomeric mutants in *E. coli* polar lipid proteoliposomes (Fig 5). The monomeric mutant BetP-W101A/T351A accumulates betaine up to approximately 250 nmol/mg protein, which is lower than the approximately 435 nmol/mg protein maximum for wild-type BetP (Fig 5A). Wild-type BetP is activated on an increase of external osmolality in the presence of internal K^+ (Peter *et al*, 1998; Fig 5B). By contrast, the mutants BetP-W101A/T351A and BetP-W101A/F345A/T351A have lost the ability to become activated in response to an increase of the external osmolality (Fig 5B).

Table 2 | Kinetics parameters of WT BetP and BetP-W101A/T351A

	K_m (μM)	V_{max} (nmol/min × mg cdw)
WT BetP	13.2 ± 5.0	185.7 ± 10.2
BetP-W101A/T351A	7.7 ± 2.7	23.6 ± 1.7

cdw, cell dry weight; WT, wild-type.

As mentioned above, the C-terminal domain of BetP is a crucial element of activity regulation. However, truncation of the C-terminal domain does not affect trimerization (Ott *et al*, 2008; Tsai *et al*, 2011; Fig 2). BetPΔC is not activated in response to osmotic shock (Fig 5B), in agreement with previous studies (Schiller *et al*, 2004a). Similarly, the monomeric mutants BetPΔC-W101A/T351A and BetPΔC-W101A/F345A/T351A also did not respond to increased osmolality (Fig 5B). To confirm that the loss of regulatory properties observed for the monomeric BetP mutants is not due to solubilization and reconstitution, the same functional measurements were recorded in MKH13 *E. coli* cells expressing monomeric BetP. Transport activation measurements were fully consistent with those in proteoliposomes. Cells expressing monomeric mutants of BetP accumulate betaine (supplementary Fig S6A online), but did not show an increased rate of uptake after an increase in osmolality (supplementary Fig S6B online). BetP-T351A, which is mainly trimeric with approximately 18% dimers (supplementary Fig S4 online), shows reduced activity at higher osmolalities. By contrast, the monomeric mutants BetP-L330A/N331A/L341A, BetPΔC-W101A/T351A and BetPΔC-W101A/F345A/T351A were not regulated by osmotic shock (supplementary Fig S6B and S7 online). We note that although the transport activity of the monomeric mutants of BetP is low, it is still significant, as shown by comparison of their activation profiles to that of an inactive mutant W377A (supplementary Fig S6B online, Ressl *et al*, 2009). Moreover, the K_m values of wild-type BetP and BetP-W101A/T351A were similar (Table 2, supplementary Fig S6C and D online).

Taken together, our results indicate that the functional unit for transport of BetP is the monomer, and that disrupting either of the inter-protomer contact networks observed in the structure (Fig 1)—e.g., by deletion of the C-terminal domain or by preventing trimerization—abolishes the ability of BetP to be activated by increased osmolality.

DISCUSSION

The protomer of a secondary transporter is generally assumed to be the functional transporting unit, whereas oligomerization is often a structure-stabilizing process (Van Dort *et al*, 2001). The possibility of a functional role for an oligomeric state has only been addressed for a few transporters because obtaining and investigating the monomeric form of an otherwise stable oligomer is difficult. Recently, the successful monomerization of the Cl^-/H^+ exchanger CLC-ec1 from *E. coli* (Robertson *et al*, 2010) provided structural and functional evidence that the monomer is the functional unit for transport. For the sodium/proton antiporter NhaA, the functional unit has been shown to be the monomer, while dimerization was found to be beneficial under stress conditions (Rimon *et al*, 2007; Herz *et al*, 2009). A dimeric state was assigned as the functional unit of the small multidrug transporter EmrE on the basis of negative-dominance studies on a genetically fused protomer tandem (Steiner-Mordoch *et al*, 2008). In the case of the multidrug transporter AcrB, the trimeric form apparently facilitates functional cooperativity of the protomers (Murakami *et al*, 2004, 2006; Eicher *et al*, 2009).

BetP was shown to be a stable trimer in the membrane of two-dimensional crystals (Tsai *et al*, 2011) and in three-dimensional crystals in the presence of detergent (Ressl *et al*, 2009). Specific functional roles for the BetP trimer could be inferred by the various inter-protomer contacts found in the three-dimensional structural data. Moreover, in two-dimensional crystals, individual protomers within one trimer were found to adopt distinct conformations, which correspond to specific states in the alternating-access cycle (Tsai *et al*, 2011). As this conformational asymmetry has been observed both in the presence and absence of the C-terminal domain (that is, the key requisite for regulation), it has been interpreted as reflecting functional coupling between the protomers during the catalytic cycle rather than during regulation, although the mechanism and functional consequences of this coupling are unknown (Tsai *et al*, 2011).

Here, we have shown that the core ‘transporting unit’ is the BetP protomer. One possible mechanism of coupling between such independent units would be cooperativity in their substrate binding, which should be reflected by lower affinities in the monomeric mutant compared with those in the trimer. However, the monomeric and trimeric forms have similar K_m values (Table 2). Instead, the catalytic turnover rate and the resultant accumulation of betaine were found to be slower in the monomer and in partly dimeric T351A (supplementary Fig S4 online; supplementary Table S2 online) compared with the trimeric versions of the protein—BetP-WT, BetP-W101A and BetP-F345A (Table 2)—supporting the hypothesis that there is conformational coupling in the catalytic cycle when BetP is trimeric. In addition to the role of the trimer in transport, the crystal structure of BetP also indicates a role for the trimeric state in the mechanism for regulation. Specifically, the structure shows that the C-terminal domain can interact with cytoplasmic loops in adjacent protomers; these loops are directly connected to helices that undergo essential conformational changes during substrate translocation (Ressl *et al*, 2009). Thus, interaction with the C-terminal domain probably restricts the flexibility of the cytoplasmic loops, which might result in transport inactivation in that particular protomer. Biochemical studies also support the presence of this cytoplasmic interaction network, although those data cannot distinguish between inter-protomer and intra-protomer interactions (Ott *et al*, 2008).

Our findings show that monomeric BetP is not regulated, even when the C-terminal domain is present, suggesting that the C-terminal domain is not interacting with the cytoplasmic loops of the same protomer. As a trimer lacking the C-terminal domains is also not regulated, these data show that regulation of activity can occur only if three monomers with intact C-terminal domains assemble together. Apparently, the long C-terminal domain itself does not have an essential role in trimerization, and the key interactions are instead located on the periplasmic side. However, these periplasmic interactions seem to be more than simply a prerequisite for enabling the C-terminal domain to interact with the cytoplasmic loops. The partly dimeric mutant BetP-T351A also shows a significantly reduced regulation profile and a reduced V_{max} compared to the wild-type protein (Table 2; supplementary Table S2 online). The implication being that even without disrupting the trimer or the cytoplasmic interaction network, partial destabilization of the periplasmic interaction at L7 (which connects h7 to TM8) is sufficient to alter the regulatory cross-talk in BetP. However, at some point, the catalytic and regulatory cycles begin to overlap. Although the monomer is the minimal functional unit for the catalytic cycle, regulation of BetP requires it to be trimeric.

METHODS

Molecular-dynamics simulations. Molecular-dynamics simulations were carried out on the X-ray structure of BetP (Protein Data Bank entry 2WIT; Ressl *et al*, 2009). The protein was inserted into a POPG bilayer according to Faraldo-Gómez *et al* (2002). Three independent simulations of either 30 or 50 ns in length were run for the trimer and monomer systems, respectively, using different initial velocities. Further details are provided in the supplementary information online.

In silico **alanine scanning.** Mutations destabilizing protomer–protomer interactions in BetP were identified by *in silico* alanine scanning using the Robetta server (Kortemme & Baker, 2002, 2004). Calculations were performed on either the X-ray structure (Ressl *et al*, 2009) or on 27 snapshots extracted from three independent molecular-dynamics trajectories of BetP trimers at equal (10 ns) time intervals.

Reconstitution of BetP. Functional reconstitution was performed as described previously (Ott *et al*, 2008).

BN–PAGE. BN–PAGE was carried out as described by Schägger and group (Wittig *et al*, 2006) with 4–12% polyacrylamide Tris Glycine gels (Invitrogen).

Size-exclusion chromatography. Protein in 50 mM Tris–HCl (pH 7.5), 200 mM NaCl, 8.7% glycerol and 0.05% DDM was loaded onto a Superdex 200 10/30 (GE Healthcare) size-exclusion column previously equilibrated with 20 mM Tris–HCl (pH 7.5), 200 mM NaCl and 0.05% DDM. All runs were performed at a flow rate of 0.2 ml/min.

Freeze-fracture electron microscopy. Freeze-fracture replicas were prepared from proteoliposomes subjected to ultra-rapid cooling into liquid ethane. Frozen samples were fractured at the same time in a Bal-Tec BAF060 instrument at 1.5×10^{-7} torr. Replicas were exanimate under a Philips EM208 S electron microscope.

Crosslinking. We performed crosslinking with glutaraldehyde on purified proteins in buffer 150 mM KPi (pH 7.5), 200 mM NaCl and 0.05% DDM. A volume of 100 μl of protein 0.25 mg/ml was treated with 0.13% glutaraldehyde; the reaction was terminated by the addition of 10 μl of 1 M Tris–HCl (pH 8.0). Site-directed intermolecular crosslinking was conducted *in situ* on membrane vesicles of *E. coli* cells. A measure of 300 μg of protein was incubated for 30 min at 25 °C and gently shaken with 5 mM of a freshly prepared crosslinkers—o-phenylenedimaleimide or *bis*-maleimidoethane—dissolved in DMSO. The reaction was terminated by addition of DTT at a final concentration of 20 mM.

Transport assays. Uptake of [^{14}C]-betaine (Moravek Biochemicals and Radiochemicals, USA) in *E. coli* cells and proteoliposomes was performed as described previously (Ott *et al*, 2008). The betaine uptake rate was calculated according to Schiller *et al* (2006). The kinetic constants were derived by Michaelis–Menten curve fitting of the uptake rates compared with the substrate concentration with GraphPad Prism version 5.0c for Mac OS X, GraphPad Software (Motulsky, 1999).

Supplementary information is available at EMBO *reports* online (http://www.emboreports.org).

ACKNOWLEDGEMENTS
This work was supported by the DFG (German Research Foundation), and Collaborative Research Center 807 'Transport and Communication across Biological Membranes' (L.R.F. and C.Z.).

CONFLICT OF INTEREST
The authors declare that they have no conflict of interest.

REFERENCES
Eicher T, Brandstätter L, Pos KM (2009) Structural and functional aspects of the multidrug efflux pump AcrB. *Biol Chem* **390:** 693–699
Faraldo-Gómez JD, Smith GR, Sansom MS (2002) Setting up and optimization of membrane protein simulations. *Eur Biophys J* **31:** 217–227
Farwick M, Siewe RM, Kramer R (1995) Glycine betaine uptake after hyperosmotic shift in *Corynebacterium glutamicum*. *J Bacteriol* **177:** 4690–4695
Forrest L, Krämer R, Ziegler C (2011) The structural basis of secondary active transport mechanisms. *Biochim Biophys Acta* **1807:** 167–188
Herz K, Rimon A, Jeschke G, Padan E (2009) β-Sheet-dependent dimerization is essential for the stability of NhaA Na^+/H^+ antiporter. *J Biol Chem* **284:** 6337–6347
Kortemme T, Baker D (2002) A simple physical model for binding energy hot spots in protein–protein complexes. *Proc Natl Acad Sci USA* **99:** 14116–14121
Kortemme T, Baker D (2004) Computational design of protein–protein interactions. *Curr Opin Chem Biol* **8:** 91–97
Motulsky H (1999) *Analyzing Data with GraphPad Prism*. GraphPad Software Inc., San Diego, CA, USA. www.graphpad.com
Murakami S, Tamura N, Saito A, Hirata T, Yamaguchi A (2004) Extramembrane central pore of multidrug exporter AcrB in *Escherichia coli* plays an important role in drug transport. *J Biol Chem* **279:** 3743–3748
Murakami S, Nakashima R, Yamashita E, Matsumoto T, Yamaguchi A (2006) Crystal structures of a multidrug transporter reveal a functionally rotating mechanism. *Nature* **443:** 173–179
Ott V, Koch J, Späte K, Morbach S, Kramer R (2008) Regulatory properties and Interaction of the C- and N-terminal domains of BetP, an osmoregulated Betaine transporter from *Corynebacterium glutamicum*. *Biochemistry* **47:** 12208–12218
Peter H, Burkovski A, Krämer R (1998) Osmosensing by N- and C-terminal extensions of the glycine betaine uptake system BetP of *Corynebacterium glutamicum*. *J Biol Chem* **273:** 2567–2574
Ressl S, Terwisscha van Scheltinga A, Vonrhein C, Ott V, Ziegler C (2009) Molecular basis of transport and regulation in the Na^+/betaine symporter BetP. *Nature* **458:** 47–52
Rimon A, Tzubery T, Padan E (2007) Monomers of the NhaA Na^+/H^+ antiporter of *Escherichia coli* are fully functional yet dimers are beneficial under extreme stress conditions at alkaline pH in the presence of Na^+ or Li^+. *J Biol Chem* **282:** 26810–26821
Robertson J, Kolmakova-Partensky L, Miller C (2010) Design, function and structure of a monomeric ClC transporter. *Nature* **468:** 844–847
Schiller D, Rübenhagen R, Krämer R, Morbach S (2004a) The C-terminal domain of the betaine carrier BetP of *Corynebacterium glutamicum* is directly involved in sensing K^+ as an osmotic stimulus. *Biochemistry* **43:** 5583–5591
Schiller D, Ott V, Krämer R, Morbach S (2006) Influence of membrane composition on osmosensing process of the betaine carrier BetP from *Corynebacterium glutamicum*. *J Biol Chem* **281:** 7737–7746
Steiner-Mordoch S, Soskine M, Solomon D, Rotem D, Gold A, Yechieli M, Adam Y, Schuldiner S (2008) Parallel topology of genetically fused EmrE homodimers. *EMBO J* **27:** 17–26
Tsai CJ, Khafizov KF, Hakulinen J, Forrest LR, Krämer R, Kühlbrandt W, Ziegler C (2011) Structural asymmetry in a trimeric Na(+)/betaine symporter BetP from *Corynebacterium glutamicum*. *J Mol Biol* **407:** 368–381
Van Dort H, Knowles D, Chasis J, Lee G, Mohandas N, Low P (2001) Analysis of integral membrane protein contributions to the deformability

and stability of the human erythrocyte membrane. *J Biol Chem* **276:** 46968–46974
Wittig I, Braun HP, Schägger H (2006) Blue native PAGE. *Nat Protoc* **1:** 418–428
Yamashita A, Singh SK, Kawate T, Jin Y, Gouaux E (2005) Crystal structure of a bacterial homologue of Na^+/Cl^- dependent neurotransmitter transporters. *Nature* **437:** 215–223
Ziegler C, Morbach S, Schiller D, Krämer R, Tziatzios C, Schubert D, Kühlbrandt W (2004) Projection structure and oligomeric state of the osmoregulated sodium/glycine betaine symporter BetP of *Corynebacterium glutamicum*. *J Mol Biol* **337:** 1137–1147
Ziegler C, Bremer E, Krämer R (2010) The BCCT family of carriers: from physiology to crystal structure. *Mol Microbiol* **78:** 13–34